Int. Rev. Appl. Sci. Eng. 8 (2017) 1, 57–65
DOI: 10.1556/1848.2017.8.1.9

DETERMINATION OF ENTRY LENGTH OF A FLUIDIZED BED DRYER USING VOLUMETRIC HEAT TRANSFER COEFFICIENT

T. POÓS[a], *V. SZABÓ*[b]

Department of Building Services and Process Engineering, Budapest University of Technology and Economics,
H-1111 Budapest, Műegyetem rakpart 3–9, Hungary
[a] E-mail: poos@mail.bme.hu
[b] E-mail: szabo.viktor@mail.bme.hu

Fluidized bed dryers are widely used in several fields of industry. Sufficiently accurate thermal models provide an opportunity to increase the effectiveness of dryers. The required size of a fluidized bed dryer can be defined with the application of mathematical model. This work is aimed at developing mathematical model to investigate the influence of operating parameters in a fluidized bed dryer using volumetric heat transfer coefficient. After the defining the input parameters of the differential equations, the required entry length of the dryer which effective heat and mass transfer between gas and particles takes place can be estimated. The correct estimation of the entry length is useful in optimal design of a fluidized bed dryer. Using the model the impact of the drying parameters can be determined to the required length.

Keywords: *fluidized bed dryer, heat and mass transfer, volumetric heat transfer coefficient, mathematical model*

1. Introduction

Heat transfer is widely used to remove moisture from a wet solid by diffusing the liquid into the vapor state. In most drying operations, water is the liquid that is evaporated, air is the normally employed purge gas.

During convectional drying simultaneous heat- and mass transfer occurs between the wet material and the drying gas. Heat transfers from the drying gas to the material and at the same time, the moisture diffuses from the material to the drying gas. Fluidized bed dryers are used for particles with small and unique geometry.

There are several types of fluidized bed dryers for industrial purposes. The most common classification is based on the mode of heat input. The heat is needed for drying the material at least with one of the following methods:

- radiation drying,
- convective drying (using drying gas),
- contact drying (by conduction from a surface that is in direct contact with the material to be dried) [1].

Fixed bed is if a fluid is passed upward through a bed of fine particles, the fluid merely percolates through the void spaces between stationary particles. In gas-solid systems, increasing the flow rate of the air beyond minimum fluidization velocity, large instabilities with bubbling and channeling of gas are observed. At higher flow rates, agitation becomes more violent and the movement of solids becomes more intensive, like a vigorously boiling liquid. The upper surface of the bed disappears, entrainment becomes appreciable, turbulent motion of solids clusters and voids of gas of various sizes and shapes are observable. With a further increase of gas velocity, solids are carried out from the tube with the gas [2]. Scaling of fluidized bed dryers as compared to other form dryers are more complex due to intense mixing of phases and the heterogeneous behavior of the bed. The heterogeneity is due to the presence of different phases such as emulsion phase, bubble phase and cloud phase with the exchange simultaneous of heat- and mass transfer between these phases [3].

1.1. Bubbling bed model

Early investigators [4] identified that the fluidized bed has to be treated as a two-phase system contains an emulsion phase and bubble phase (often called as dense and lean phases). The bubbles contain very

This is an open-access article distributed under the terms of the Creative Commons Attribution-NonCommercial 4.0 International License (https://creativecommons.org/licenses/by-nc/4.0/), which permits unrestricted use, distribution, and reproduction in any medium for non-commercial purposes, provided the original author and source are credited, a link to the CC License is provided, and changes – if any – are indicated.

© 2017 The Author(s)
ISSN 2062-0810

Unauthenticated | Downloaded 12/02/23 05:27 AM UTC

small amounts of solids. They have an approximately hemispherical geometry on the top and a pushed-in bottom. Each bubble of gas has a wake which contains a significant amount of solids. The gas within a particular bubble remains largely within that bubble, penetrating only a short distance into the surrounding emulsion phase. This region penetrated by gas from a rising bubble called as cloud.

The three-phase back-mixing (bubbling bed) model was developed by Kunii and Levenspiel [2]. The bubbling bed consists of three distinct phases such as bubble phase, cloud-wake phase and emulsion of dense solid phase. There are some assumptions and limitations of the model:

- In the bubble phase, gas moves upward as a plug flow.
- In the cloud-wake phase, gas moves upward along with bubbles.
- In the emulsion or dense phase, solids move downward.
- The moisture and temperature distributions of the emulsion and solids phase are uniform over the bed, but have distribution for bubble phase.
- Solids do not tend to agglomerate.
- All particle interaction is ignored, implying that any heat and mass transfer between individual particles and the emulsion phase.
- No attempt is made to allow for particle size distribution.
- The wall of the bed is insulated and there is no heat transfer between the wall and the interstitial gas and solids phases [5].

Some authors [6, 7] use the theory of bubbling bed model for the completion of numerical simulations, where the heat transfer characteristics are well examinable. There are heat and mass transfer between the phases, as:

- transfer from gas in the bubble to solids in the bubble phase,
- transfer from bubble phase to cloud phase,
- transfer from gas in cloud to solid phase,
- transfer from cloud phase to emulsion phase,
- transfer from gas in emulsion phase to solid [1].

The practical use of bubbling bed model is fairly difficult to evaluate laboratory measurements due the hard measureable parameters, e.g. diameter of bubbles. Hereafter we will treat the fluidized bed as two-phase model contains solid and gas phases, assumed flow around sphere.

1.2. Nu–Re *relationship*

This approach relates transfer coefficients to the dimensionless numbers, which are evaluated using a wide range of experimental data. In the literature there are several $Nu = f(Re)$ equations using the characterization to heat transfer between solids and drying gas. These are necessary to scale up fluidized bed dryers using for a process.

Since the middle of the 20th century, when the first commercial fluidized bed was installed, hundreds of fluidized bed dryers have been used worldwide to dry a wide range of materials, particularly granular materials which can be readily fluidized [8]. Despite the widespread application of fluidized bed dryers, the development of efficient and reliable modelling tools has been undermined by lack of systematic and well-documented data the literature [9].

The basics of the scaling up procedure is the determination of the required minimal entry length above the distributor plate of the fluidized bed. This is important in designing the dryer equipment to reduce the pressure drop of the fluidized bed and decreasing the power consumption in the process. In a fluidized bed, the gas-particle heat and mass transfer takes place only up a certain length called the entry length [10]. Under steady state the hot gas enters the bed than cooled by the cold solids, and simultaneously, the entering dry gas absorbs moisture from the wet particles. Along the length of the fluidized bed, the temperature of gas continuously decreases, and the absolute humidity of the gas increasing, until reaching the saturation state. On the saturation state the temperature of drying gas tends to the wet bulb temperature, while the humidity tends to the saturation absolute humidity. Above this point the drying gas is not able to carry more moisture from the particles, so during the scaling up this length should be determined. The absolute humidity, and temperature profile of the drying gas along the fluidized bed represented in Fig. 1 under steady state. The required entry length marked with Z, the inlet temperature with $T_{G,\mathrm{in}}$, the absolute humidity with $Y_{G,\mathrm{in}}$, and the saturation (wet bulb) temperature is $T_{G,\mathrm{sat}}$, and the saturation absolute humidity with $Y_{G,\mathrm{sat}}$.

In the literature there are number of methods to evaluate the entry length. Walton et al. [11] examined

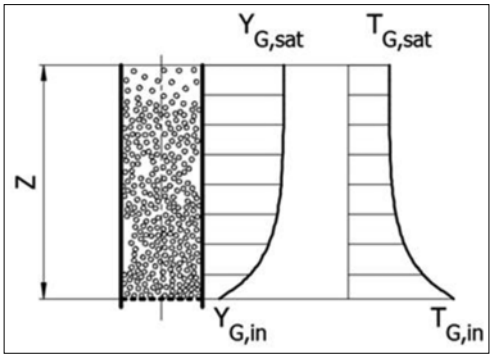

Fig. 1. The absolute humidity and temperature profiles of drying gas along the length of the fluidized bed

Unauthenticated | Downloaded 12/02/23 05:27 AM UTC

the heat transfer characteristics in a fluidized bed in batch operation. They assumed uniform bed temperature for the solid, and they neglected the heat loss through the walls. The slope of the temperature of drying gas can be calculated at any point through the length of the dryer:

$$\frac{dT_G}{dz} = -\frac{\alpha a}{c_G \dot{m}_{dG}}\left(T_G - T_P\right), \tag{1}$$

where dz is the elementary length coordinate, α is the heat transfer coefficient, a is the volumetric interfacial surface area, c_G is the specific heat of gas, $\dot{m}_{dG}$ is the mass flow rate of gas, T_G is the temperature of gas, and T_P is the temperature of material.

Roy et al. [10] determined the entry length of a fluidized bed granulator using Stanton number:

$$Z = -\frac{cd_P}{6St\left(1-\varepsilon\right)}, \tag{2}$$

where d_P is the particle diameter, St is Stanton number, and ε is the porosity of bed. Constant c is defined as the follow expression:

$$e^{-c} = \frac{T_G - T_P}{T_{G,in} - T_P}. \tag{3}$$

Ng et al. [12] optimized an industrial-scale fluidized bed dryer using Class 1 and Class 3 models, drying GeldartType D nylon particles. Assuming plug-flow behavior and neglecting the influence of the bubble phase, the Class 1 model can be used. The minimum bed height needed to ensure that the moisture content in exit air is maximized, i.e. at adiabatic saturation can be calculated with the following equation:

$$Z = \frac{\rho_G c_G v}{\alpha a} \ln\left(\frac{Y_{G,\mathrm{sat}} - Y_{G,\mathrm{in}}}{Y_{G,\mathrm{sat}} - Y_G}\right), \tag{4}$$

where ρ_G is the density of gas, c_G is the specific heat of gas, v is the superficial gas velocity.

Using Class 3 model, the humidity content of the dense phase along the bed height:

$$\frac{\mathrm{d}Y_d}{\mathrm{d}z} = \left(Y_{G,\mathrm{sat}} - Y_d\right)\left(\frac{\alpha a}{\rho_G c_G v_d}\right) - \sigma_c \frac{6}{d_P}\frac{1}{u_b}\left(Y_d - Y_b\right), \tag{5}$$

where Y_d is the absolute humidity of dense phase, σ_c is the mass transfer coefficient between bubble and dense phase, v_d is the average velocity in dense phase, v_b is the velocity of bubbles, and Y_b is the absolute humidity of bubble phase.

The heat transfer coefficient between gas and particles is calculated in the literature dealing with the scaling-up is calculated from various $Nu = f(Re)$ criterial equations. The heat transfer coefficient can be calculated by making some simplifying assumptions, meaning to assume that the geometry of the particles is spherical, and the contact between the gas and the material is ideal, which means that during the drying process each particle is in contact with the drying gas, on its whole surface. With these assumptions, and in the knowledge of the total number of particles in the drying chamber, the contact surface of the material can be determined [13].

The volumetric interfacial surface area is calculated in those literatures knowing the porosity of particles, sphericity and assuming that the particles are spherical [14]:

$$a = \frac{6\left(1-\varepsilon\right)\Phi}{d_P}, \tag{6}$$

where Φ is the sphericity.

Application of a volumetric heat transfer coefficient (αa) and modified dimensionless numbers for mathematical models provides favorable opportunities to describe the drying process of wet particles, and eliminates the above-mentioned uncertainties in the heat transfer area [15]. The mathematical models of fluidized bed drying require the volumetric heat transfer coefficient between the gas and particles. A volumetric heat transfer coefficient was applied for modeling fluidized bed dryers in our previous work. Based on our measurements and literature data a modified $Nu' = f(Re)$ relationship was created for fluidized bed drying [16]:

$$Nu' = 7.2 \cdot 10^{-4} \cdot Re^{1.68}. \tag{7}$$

The purpose of our work is to determine the required entry length of the fluidized bed dryer using volumetric heat transfer coefficient as an input parameter to the mathematical model.

1.3. Scheme of the dryer

Mathematical model was developed for fluidized bed dryers in batch operation. Figure 2 shows the sketch of the fluidized bed dryer presented the gas- and material flow, the main properties of gas and material, and the position of drying particles during the operation. Figure 2a shows the position of the particles after the conveying, and the static bed height (L_0) is measured by scale. The material has known mass (m_P) and moisture content (X_{in}). According to Fig. 2b after the chamber is loaded, the drying gas enters to the chamber through a grid with known mass flow rate ($\dot{m}_{dG}$), temperature ($T_{G,\mathrm{in}}$), and absolute humidity ($Y_{G,\mathrm{in}}$). The gas exits the chamber with the same mass flow rate, and its temperature ($T_{G,\mathrm{out}}$), and absolute humidity ($Y_{G,\mathrm{out}}$) can be measured. The surface temperature (T_P) of material is

Unauthenticated | Downloaded 12/02/23 05:27 AM UTC

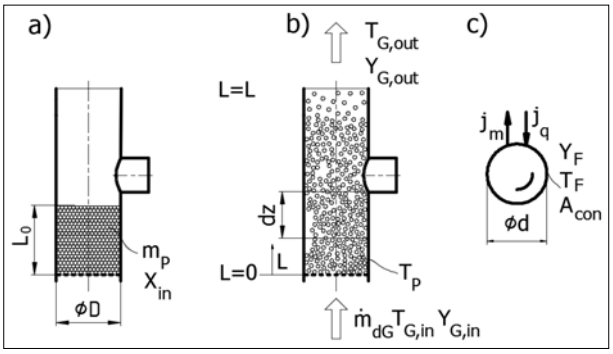

Fig. 2. Sketch of the dryer. a) Sketch of the static bed. b) Sketch of the dynamic bed. c) Sketch of one particle represented the convective heat and mass flux

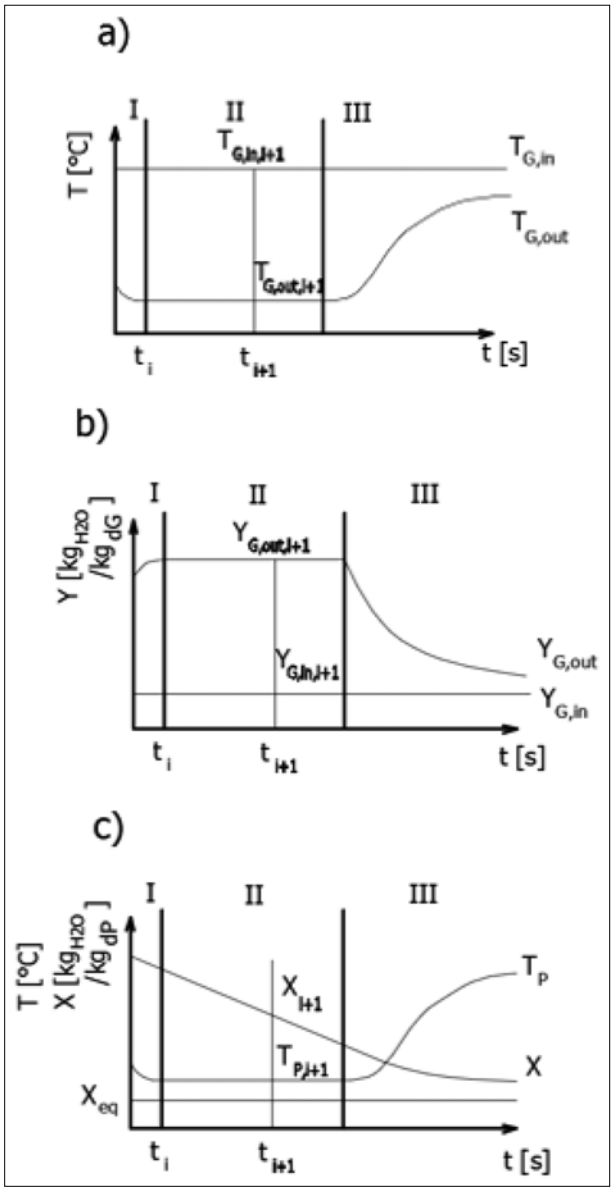

Fig. 3. Drying curves. a) $T_{G,\text{in}} = f(t)$, $T_{G,\text{out}} = f(t)$, b) $Y_{G,\text{in}} = f(t)$, $Y_{G,\text{out}} = f(t)$, c) $T_P = f(t)$, $X = f(t)$

measured with infrared thermometer. The total length of the dynamic fluidized bed marked with L. During convectional drying, simultaneous heat and mass transfer occurs between the wet material and the drying gas (Fig. 2c). During the constant drying rate period the gas saturated around the particles, which can be characterized by saturated absolute humidity (Y_S) and the surface temperature of particles tends to wet bulb temperature.

The drying curves of fluidized bed are shown in Fig. 3. Figure 3a shows the vary of the inlet and outlet temperature of gas, Fig. 3b shows the inlet and outlet absolute humidity of gas, and Fig. 3c shows the moisture content and temperature of particles in the function of time. The time interval of starting period (I period) is negligible compared to the total drying time. This section lasts until the surface temperature of the material will be constant. During the constant drying rate period (II period) the surface humidity evaporates to the drying gas, the temperature of the material is constant, and it is equal to the wet-bulb temperature. The moisture content of particles decreases, the drying gas deemed to be saturated. During the falling drying rate period (III period) dry spots can be observed on the surface of the material, and the moisture exhausts from the pores and capillaries. The moisture content of the wet particles decreases and tends to the equilibrium moisture content, and the surface temperature increases. The humidity of drying gas begins to decrease due to the falling drying rate [17].

2. Materials and methods

The modelling is formulated with the following terms:

– The fluidized bed is perfectly mixed, so the temperature (T_P) and moisture content (X) of the particles are constant along the dryer.

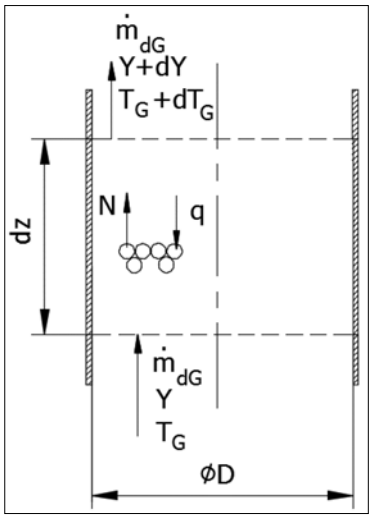

Fig. 4. Heat and mass transfer, and gas flow in a short section of the dryer

Unauthenticated | Downloaded 12/02/23 05:27 AM UTC

- The temperature and moisture content distribution inside the particles are negligible.
- The surface temperature of particles can be measured with good approximation the same as the temperature inside the particles, so $T_S \approx T_P$.
- The drying material is geometrically homogeneous (does not shrinking and no deformation).
- The mass flow rate of the drying gas is constant during the operation.
- The heat loss and radiation are negligible.
- No chemical reactions take place during the drying.

Figure 4 shows the direction of heat and mass transfer and the gas flow in a short section of the fluidized bed dryer in batch operation.

2.1. Variation of the absolute humidity of gas

Humidity balance of the drying gas for a section $\mathrm{d}z$, in a moment:

$$\dot{m}_{dG} Y + N \mathrm{d}A_{con} = \dot{m}_{dG} \left(Y + \mathrm{d}Y \right), \tag{8}$$

Equation (8) can be reduced:

$$\dot{m}_{dG} \mathrm{d}Y = N \mathrm{d}A_{\mathrm{con}}. \tag{9}$$

Drying rate with the gas-side driving force:

$$N = \sigma \left(Y_F - Y \right). \tag{10}$$

Substituting Eq. (10) into Eq. (9) we get:

$$\mathrm{d}Y = \frac{\sigma \left(Y_F - Y \right)}{\dot{m}_{dG}} \mathrm{d}A_{\mathrm{con}}. \tag{11}$$

The volumetric contact surface area between the gas and material on section $\mathrm{d}z$, on the full length of static bed [17]:

$$a = \frac{\mathrm{d}A_{\mathrm{con}}}{A_d \mathrm{d}z} = \frac{A_{\mathrm{con}}}{A_d L_0}. \tag{12}$$

Substituting Eq. (6) into Eq. (7) we get the variation in the absolute humidity of drying gas along the length of the dryer:

$$\frac{\mathrm{d}Y}{\mathrm{d}z} = \frac{\sigma a A_d}{\dot{m}_{dG}} \left(Y_F - Y \right). \tag{13}$$

Using $\mathrm{d}z = v_G \mathrm{d}t$ we get the variation in the absolute humidity of drying gas at elementary time intervals:

$$\frac{\mathrm{d}Y}{\mathrm{d}t} = \frac{\sigma a A_d v_G}{\dot{m}_{dG}} \left(Y_F - Y \right). \tag{14}$$

The connection between heat and mass transfer has been analyzed by a number of authors [17, 18], applying various methods for description. In case of gas flow through a granulate layer, the shape resistance is negligible compared to friction resistance, therefore the analogy of heat, mass, and momentum transfer can be applied. Based on similarities of temperature, concentration, and velocity profiles, the heat transfer and mass transfer factors [16]: $j_q = j_m$. Based on the interpretation of the heat and mass transfer factors:

$$j_q = \frac{Nu}{RePr} Pr^z = \frac{Sh}{ReSc} Sc^z = j_m. \tag{15}$$

It can be deduced:

$$\frac{\alpha}{k_c \rho c_G} = \left(\frac{Sc}{Pr} \right)^z = Le^z. \tag{16}$$

In case of air–water system $Le^z \approx 1$, the following correlation can be stated using $\sigma = k_c \rho_G$:

$$\frac{\alpha}{k_c \rho} = \frac{\alpha}{\sigma} = c_G. \tag{17}$$

Assembling Eq. (13) and Eq. (17) the variation in the absolute humidity of drying gas with volumetric heat transfer coefficient:

$$\frac{\mathrm{d}Y}{\mathrm{d}z} = \frac{\alpha a}{c_G} \frac{A_d}{\dot{m}_{dG}} \left(Y_F - Y \right), \tag{18}$$

and finally:

$$\frac{\mathrm{d}Y}{\mathrm{d}t} = \frac{\mathrm{d}Y}{\mathrm{d}z} v_G = \frac{\alpha a}{c_G \rho_G} \left(Y_F - Y \right). \tag{19}$$

2.2. Variation of the moisture content of material

The fluidized bed is perfectly mixed, therefore the variation in the moisture content of material along the bed height is negligible. The mass balance equation shows the connection between the amount of water evaporated from the material and the amount of humidity taken by the drying gas during the drying process:

$$\frac{-\dot{m}_{dP} \mathrm{d}X}{\mathrm{d}t} = \dot{m}_{dG} \mathrm{d}Y, \tag{20}$$

The variation in the moisture content of the drying material can be deduced:

$$\frac{\mathrm{d}X}{\mathrm{d}t} = -\frac{\dot{m}_{dG}}{m_{dP}} \mathrm{d}Y. \tag{21}$$

2.3. Variation of the temperature of drying gas

The enthalpy flow-balance of the drying gas for a section $\mathrm{d}z$, in a moment:

$$\begin{aligned} &\dot{m}_{dG} h_G + N h_{v,F} \mathrm{d}A_{\mathrm{con}} \\ &\quad = \dot{m}_{dG} \left(h_G + \mathrm{d}h_G \right) + q \mathrm{d}A_{\mathrm{con}}, \end{aligned} \tag{22}$$

Unauthenticated | Downloaded 12/02/23 05:27 AM UTC

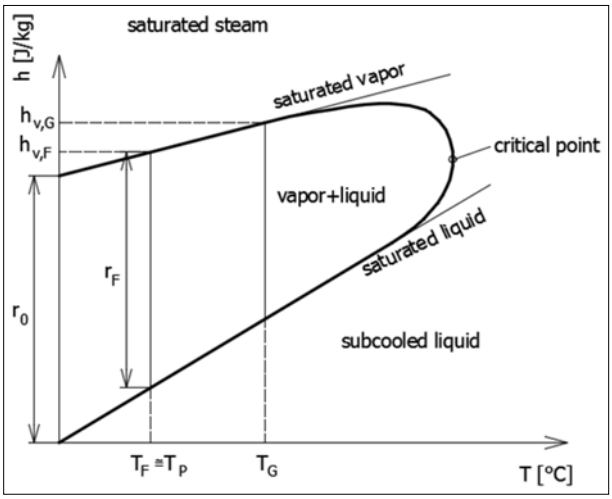

Fig. 5. Specific enthalpy–temperature diagram [19]

Equation (22) can be deduced:

$$\dot{m}_{dG}\,\mathrm{d}h_G = N h_{v,F}\,\mathrm{d}A_{\mathrm{con}} - q\,\mathrm{d}A_{\mathrm{con}}. \tag{23}$$

The contact between the specific enthalpy of liquid and vapor represented in the specific enthalpy–temperature diagram, Fig. 5 [12].

According to the *h*–*T* diagram the contact between $h_{v,F}$ and $h_{v,G}$:

$$\begin{aligned} h_{v,F} &= h_{v,G} - c_v\left(T_G - T_F\right) \\ &= r_0 + c_v T_G - c_v\left(T_G - T_F\right). \end{aligned} \tag{24}$$

The specific enthalpy of the wet gas is:

$$h_G = \frac{\dot{H}_{dG} + \dot{H}_v}{\dot{m}_{dG}} = c_{dG}T_G + Y\left(r_0 + c_v T_G\right), \tag{25}$$

derived from Eq. (25):

$$\begin{aligned} \mathrm{d}h_G &= \frac{\partial h_G}{\partial T_G}\mathrm{d}T_G + \frac{\partial h_G}{\partial Y}\mathrm{d}Y \\ &= \left(c_{dG} + Yc_v\right)\mathrm{d}T_G + \left(r_0 + c_v T_G\right)\mathrm{d}Y \\ &= c_G\,\mathrm{d}T_G + \left(r_0 + c_v T_G\right)\mathrm{d}Y. \end{aligned} \tag{26}$$

Substituting Eqs (9) and (26) in Eq. (23)

$$\begin{aligned} &\dot{m}_{dG}\left[c_G\,\mathrm{d}T_G + \left(r_0 + c_v T_G\right)\mathrm{d}Y\right] \\ &\quad = \dot{m}_{dG}\,\mathrm{d}Y h_{v,F} - q\,\mathrm{d}A_{\mathrm{con}}. \end{aligned} \tag{27}$$

Simplifying Eq. (27):

$$\dot{m}_{dG}c_G\,\mathrm{d}T_G = \dot{m}_{dG}\,\mathrm{d}Y\left(h_{v,F} - r_0 - c_v T_G\right) - q\,\mathrm{d}A_{\mathrm{con}}. \tag{28}$$

The heat flux between drying gas and material using logarithmic temperature difference:

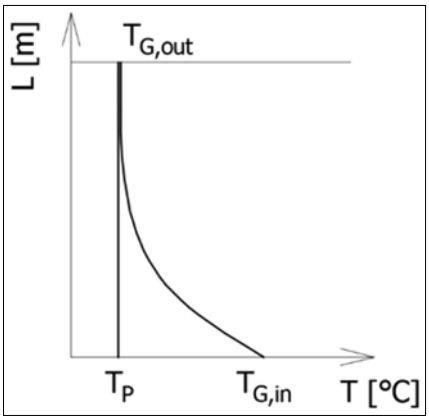

Fig. 6. Variation of the temperature of gas and material along the dryer

$$q = \alpha\Delta T_{G-P} = \alpha\frac{\left(T_{G,\mathrm{in}} - T_P\right) - \left(T_{G,\mathrm{out}} - T_P\right)}{\left(T_{G,\mathrm{in}} - T_P\right)\left(T_{G,\mathrm{out}} - T_P\right)^{-1}}. \tag{29}$$

Figure 6 illustrates the variation of the temperature of gas and material along the dryer.

Substituting Eqs (12), (24) and (29) in Eq. (28)

$$\begin{aligned} \mathrm{d}T_G = &-\frac{c_v}{c_G}\left(T_G - T_P\right)\mathrm{d}Y \\ &-\frac{1}{\dot{m}_{dG}c_G}\alpha a\,\mathrm{d}z\,A_d\,\Delta T_{G-P}. \end{aligned} \tag{30}$$

From Eq. (30) the variation in the temperature of drying gas for a section dz can be deduced:

$$\begin{aligned} \frac{\mathrm{d}T_G}{\mathrm{d}z} = &-\frac{c_v}{c_G}\left(T_G - T_P\right)\frac{\mathrm{d}Y}{\mathrm{d}z} \\ &-\frac{1}{\dot{m}_{dG}c_G}\alpha a\,A_d\,\Delta T_{G-P}, \end{aligned} \tag{31}$$

Variation in the temperature of drying gas at elementary time intervals using $\mathrm{d}z = v_G\,\mathrm{d}t$:

$$\begin{aligned} \frac{\mathrm{d}T_G}{\mathrm{d}t} &= -\frac{c_v}{c_G}\left(T_G - T_P\right)\frac{\mathrm{d}Y}{\mathrm{d}t} - \frac{\alpha a}{\dot{m}_{dG}c_G}v_G A_d\,\Delta T_{G-P} \\ &= -\frac{c_v}{c_G}\left(T_G - T_P\right)\frac{\mathrm{d}Y}{\mathrm{d}t} - \frac{\alpha a}{c_G\rho_G}\Delta T_{G-P}. \end{aligned} \tag{32}$$

2.4. Variation of the temperature of material

The heat balance between the drying gas and particles contains the flux from evaporation and heating-up:

$$q = q_{\mathrm{evap}} + q_{\mathrm{heating}}. \tag{33}$$

Drying rate with the material-side driving force:

$$N = -\frac{m_{dP}}{A_{\mathrm{con}}}\frac{\mathrm{d}X}{\mathrm{d}t}r_F. \tag{34}$$

Unauthenticated | Downloaded 12/02/23 05:27 AM UTC

Equation (33) can be expanded using Eqs (29) and (34)

$$\alpha \Delta T_{G-P} = \frac{m_{dP} c_P}{A_{\text{con}}} \frac{\mathrm{d}T_P}{\mathrm{d}t} - \frac{m_{dP}}{A_{\text{con}}} \frac{\mathrm{d}X}{\mathrm{d}t} r_F. \qquad (35)$$

Rearranging Eq. (31)

$$\frac{\mathrm{d}T_P}{\mathrm{d}t} = \frac{A_{\text{con}}}{m_{dP} c_P} \left(\alpha \Delta T_{G-P} + \frac{m_{dP}}{A_{\text{con}}} \frac{\mathrm{d}X}{\mathrm{d}t} r_F \right). \qquad (36)$$

Variation in the temperature of the drying product at elementary time intervals substituting Eq. (12) in Eq. (36)

$$\frac{\mathrm{d}T_P}{\mathrm{d}t} = \frac{\alpha a}{m_{dP} c_P} L_0 A_d \Delta T_{G-P} + \frac{r_F}{c_P} \frac{\mathrm{d}X}{\mathrm{d}t}. \qquad (37)$$

The fluidized bed is perfectly mixed, therefore the variation in the temperature of material along the bed height is negligible.

2.5. Application of the mathematical model

The mathematical models of fluidized bed drying require the volumetric heat transfer coefficient (αa) between the gas and particles. A volumetric heat transfer coefficient was applied for modeling fluidized bed dryers in our previous work. Based on our measurements and literature data a modified $Nu' = f(Re)$ relationship was created for fluidized bed drying [16]

$$Nu' = 7.2 \cdot 10^{-4} \cdot Re^{1.68}. \qquad (38)$$

The Reynolds and the modified Nusselt numbers are the components of the critical equations for modeling fluidized bed drying:

$$Re = \frac{v_G d}{\nu_G}; \qquad Nu = \frac{\alpha a\, d^2}{\lambda_G}. \qquad (39)$$

The input parameters of the model are listed in Table 1. The model makes it possible to calculate the temperature and absolute humidity of drying gas along the length of the fluidized bed dryer (z) as well as in the function of time (t), furthermore the temperature and moisture of the material can be calculated in the function of time (t).

The drying product was sorghum at this study. During the constant rate period ($X > X_{\text{critical}}$), saturated air was presumed at the interface. From the lower moisture content of the product $X < X_{\text{critical}}$, the relative humidity of the gas is $\varphi < 1$. The relative humidity of the gas can be obtained from the equilibrium moisture curve $\varphi = f(X)$ [19]. The moisture desorption isotherm was determined by measurements [20]. The desorption isotherm of sorghum represented in Fig. 6, which is valid between 30 °C and 70 °C.

The absolute humidity of drying gas at the material interface can be determined:

$$Y_F = \frac{M_{\text{H}_2\text{O}}}{M_{dG}} \frac{\varphi p_{v,\text{sat}}}{P - \varphi p_{v,\text{sat}}}. \qquad (40)$$

where is the molecular weight of the water, M_{dG} is the molecular weight of drying gas, φ is the relative humidity of gas, P is the absolute pressure, and $p_{v,\text{sat}}$ is the saturation gas pressure, which in the function of the saturation temperature $T_{G,\text{sat}}$. The saturated temperature (and also the saturation absolute humidity) can be determined by using Mollier diagram knowing the inlet temperature $T_{G,\text{in}}$ and absolute humidity of gas $Y_{G,\text{in}}$.

Equations (19) and (32) make it possible to calculate the absolute humidity and temperature of drying gas, and Eqs (21), (37) the moisture content and temperature of material in the function of time. The initial values at $t = 0$ are:

Table 1. Input parameters

Nominations	Values	Units
D	0.1	m
$\dot{m}_{dG}$	0.027	kg/s
$m_{dP,\text{in}}$	0.665	kg
$T_{G,\text{in}}$	70	°C
$T_{P,\text{in}}$	20	°C
X_{in}	0.58	$\text{kg}_{\text{H}_2\text{O}}/\text{kg}_{\text{dG}}$
X_{out}	0.35	$\text{kg}_{\text{H}_2\text{O}}/\text{kg}_{\text{dG}}$
αa	23950	$\text{W/m}^3\text{/K}$
d	0.034	m
L_0	0.16	m
Δz	0.05	m
Δt	0.01	s

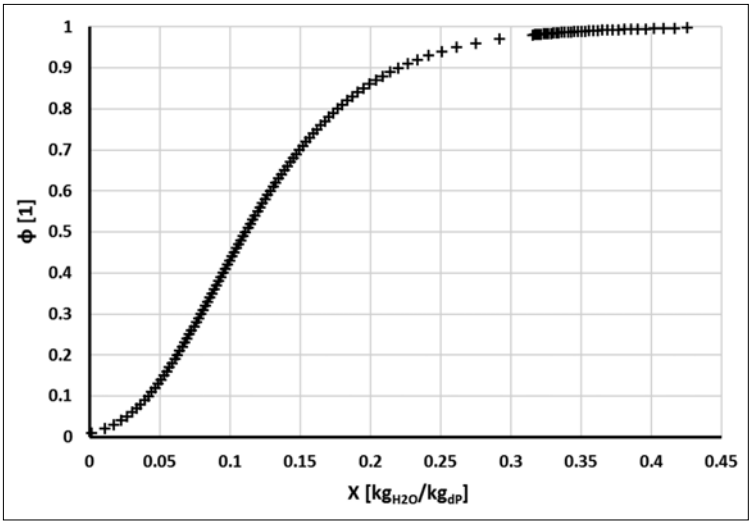

Fig. 7. Desorption isotherm of sorghum [20]

Unauthenticated | Downloaded 12/02/23 05:27 AM UTC

$$X = X_{\text{in}}; \quad Y_G = Y_{G,\text{in}}; \quad T_G = T_{G,\text{in}}; \quad T_P = T_{P,\text{in}}.$$

For every elementary time interval Δt is

$$\Delta X = \frac{\mathrm{d}X}{\mathrm{d}t}\Delta t; \quad \Delta Y_G = \frac{\mathrm{d}Y_G}{\mathrm{d}t}\Delta t;$$
$$\Delta T_G = \frac{\mathrm{d}T_G}{\mathrm{d}t}\Delta t; \quad \Delta T_P = \frac{\mathrm{d}T_P}{\mathrm{d}t}\Delta t.$$

The temperature and moisture content of the product and the temperature and absolute humidity of gas can be calculated adding the values of the elementary time intervals to the initial values:

$$X = X_{\text{in}} + \Delta X; \quad Y_G = Y_{G,\text{in}} + \Delta Y_G;$$
$$T_G = T_{G,\text{in}} + \Delta T_G; \quad T_P = T_{P,\text{in}} + \Delta T_P.$$

3. Results

By repeating the calculation step by step ($\Delta t = 0.05$ s) the drying curves can be created, and the drying time can be determined. The drying process finishes when the moisture content of material reaches the desired final moisture content. Figures 8–11 show the drying curves calculated with the mathematical model using the input parameters represented in Table 1. The volumetric heat transfer coefficient was determined from Eq. (38).

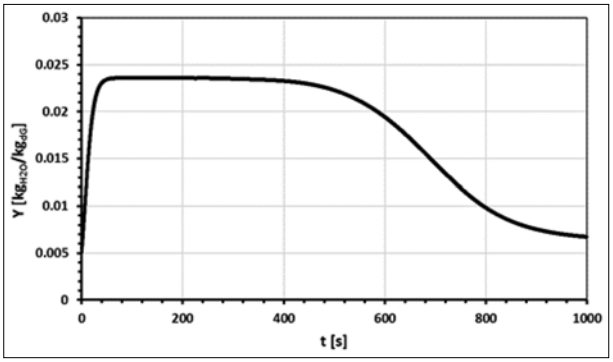

Fig. 8. Absolute humidity of gas vs drying time

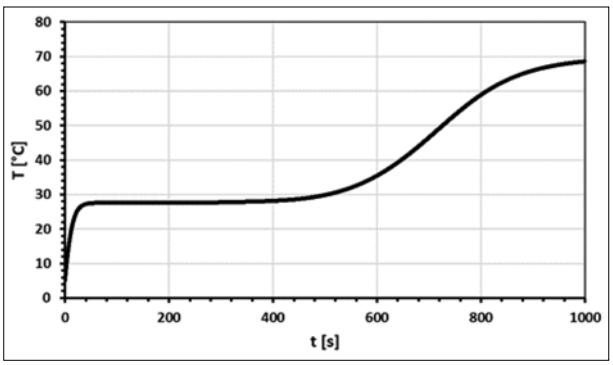

Fig. 9. Temperature of gas vs drying time

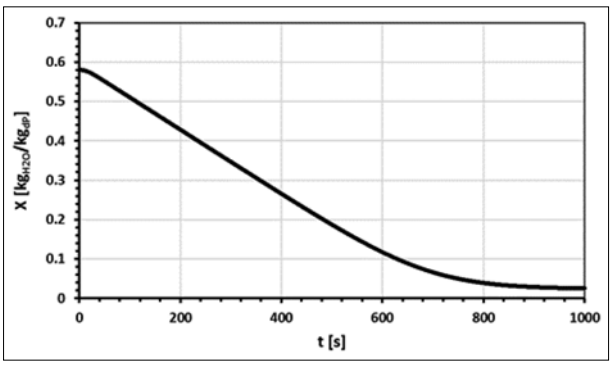

Fig. 10. Moisture content of material vs drying time

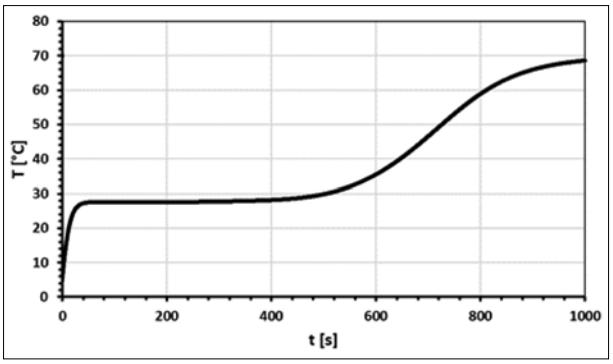

Fig. 11. Temperature of particles vs drying time

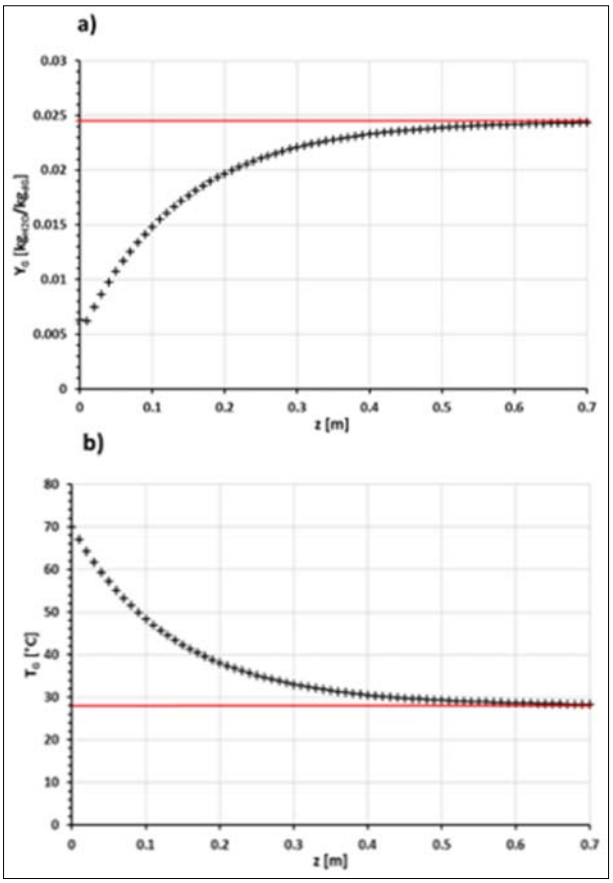

Fig. 12. Calculating the required entry length. a) Absolute humidity of drying gas vs length, b) Temperature of drying gas vs length

Unauthenticated | Downloaded 12/02/23 05:27 AM UTC

The variation of the absolute humidity of drying gas versus the time represented in Fig. 8, the temperature of drying gas in Fig. 9. From the material side the variation of the moisture content represented in Fig. 10, and the temperature of surface temperature of particles in Fig. 11.

By repeating the calculation step by step (Δz = 0.01 m) the absolute humidity and temperature curves can be created, and the required entry length can be determined. To avoid numerical failures, the calculation steps should be selected to an appropriate low resolution. Figure 12 shows the humidity and temperature curves, and the saturated values (red line). The value of volumetric heat transfer coefficient was evaluated from Eq. (38). The value of the required entry length can be determined from the diagram.

The absolute humidity of gas in every elementary steps can be calculated with the following method:

$$Y_G^{i+1} = Y_G^i + \mathrm{d}z\left[\frac{\alpha a}{c_G}\frac{A_d}{\dot{m}_{dG}}\left(Y_{G,\mathrm{sat}} - Y\right)\right]. \qquad (41)$$

4. Conclusions

The purpose of our work was to develop a mathematical model to determine the entry length for fluidized bed drying. Volumetric heat transfer coefficient is required in this model. The model made it possible to calculate the temperature and absolute humidity of drying gas versus the length of dryer. The goal of our work was to propose a new method for scaling up fluidized bed dryers using a volumetric heat transfer coefficient.

Acknowledgements

This paper was supported by Gedeon Richter's Talentum Foundation (H-1103 Budapest, Gyömrői út 19–21, Hungary), and by Hungarian Scientific Research Found (OTKA-116326).

References

[1] Syahrul S., Hamdullahpur F. et al. (2002), Exergy analysis of fluidized bed drying of moist particles. Exergy, an International Journal, 2, 87–98.
[2] Kunii D., Levenspiel O. (1991), Fluidization Engineering. 2nd ed., New York: Butterworth-Heinemann.
[3] Srinivasakannan C., Shoibi A. A. et al. (2012), Combined resistance bubbling bed model for drying of solids in fluidized beds. Heat and Mass Transfer, 48(4), 621–625.
[4] Davidson J. F., Harrison D. (1963), Fluidized Particles. New York: Cambridge University Press.
[5] Wang, H. G., Dyakowski T., et al. (2007), Modelling of batch fluidised bed drying of pharmaceutical granules. Chemical Engineering Science, 62, 1524–1535.
[6] Khorshidi J., Davari H., et al. (2011), Model making for heat transfer in a fluidized bed dryer. Journal of Basic and Applied Scientific Research, 1, 1732–1738.
[7] Rizzi Jr. A. C., Passos M. L., et al. (2009), Modeling and simulating the drying of grass seeds (Brachiariabrizantha) in fluidized beds: evaluation of heat transfer coefficients. Brazilian Journal of Chemical Engineering, 26(3), 545–554.
[8] Zahed A. H., Zhu J.-X., et al. (2007), Modelling and simulation of batch and continuous fluidized bed dryers. Drying Technology, 13, 1–28.
[9] Burgschweiger J., Tsotsas E. (2002), Experimental investigation and modelling of continuous fluidized bed drying under steady-state and dynamic conditions. Chemical Engineering Science, 57, 5021–5038.
[10] Roy P., Vashishtha M., et al. (2009), Heat and mass transfer study in fluidized bed granulation – Prediction of entry length. Particuology, 7, 215–219.
[11] Walton J. S., Olson R. L., et al. (1952), The partial coefficient of heat transfer in a drying fluidized bed. Chem. Eng. Sci., 44, 1474–1480.
[12] Ng W. K., Tan R. B. H. (2008), Case study: Optimization of an industrial fluidized bed drying process for large Geldart-type D nylon particles. Powder Technology, 180, 289–295.
[13] Kumaresan R., Viruthagiri T. (2006), Simultaneous heat and mass transfer studies in drying ammonium chloride in a batch-fluidized bed dryer. Indian Journal of Chemical Technology, 13, 440–447.
[14] Ciesielczyk W. (1996), Analogy of heat and mass transfer during constant rate period in fluidized bed drying. Drying Technology, 14, 217–230.
[15] Alvarez P. I., Shene C. (1992), Experimental determination of volumetric heat transfer coefficient in a rotary dryer. Drying Technology, 12, 1605–1627.
[16] Poós T., Szabó V. (2016), Application of volumetric heat transfer coefficient on fluidized bed dryers. 8th International Symposium on Exploitation of Renewable Energy Sources, pp. 72–75.
[17] Treybal R. E. (1981), Mass-transfer operations. 3rd ed. New York: McGraw-Hill Company.
[18] Szentgyörgyi S., Molnár K., Parti M. (1986), Transzportfolyamatok. Tankönyvkiadó, Budapest.
[19] Környey T. (2005), Termodinamika. Műegyetemi Kiadó.
[20] Poós T., Örvös M. (2012), Heat- and mass transfer in agitated co- or countercurrent, conductive–convective heated drum dryer. Drying Technology 30, 1457–1468.
[21] Aviara N. A., Ajibola O. O., et al. (2006), Moisture sorption isotherms of sorghum malt at 40 and 50 °C. Journal of Stored Product Research, 42, 290–301.
[22] Nyers J., Nyers A. (2016), Hydraulic analysis of heat pump's heating circuit using mathematical model. 9th ICCC International Conference, Proceedings-USB, Tihany, Hungary. 04-08.07. ISBN 978-1-4799-0061-9, pp. 349–353.

Unauthenticated | Downloaded 12/02/23 05:27 AM UTC